EXTENDED OPTIMIZATION STUDY AND PANEL PARAMETER STUDY FOR NOISE RADIATION REDUCTION OF AN AIRCRAFT PANEL EXCITED BY TURBULENT FLOW

Steven A.J. Sonnenberg † and Joana Rocha ‡
Department of Mechanical and Aerospace Engineering, Carleton University, Ottawa, Ontario.

Résumé

Le bruit et les vibrations dans une cabine d'aéronef en conditions de croisière sont principalement causés par des excitations extérieures d'écoulement d'air de la Couche Limite Turbulente (CLT). La CLT provoque des vibrations sur les panneaux de fuselage de l'aéronef. Ces vibrations rayonnent de l'énergie sonore sous la forme de bruit. Par conséquent, il est intéressant de déterminer quel paramètre du panneau d'aéronef est le plus susceptible de diminuer la quantité d'énergie acoustique rayonnée afin de permettre l'optimisation de ces paramètres pour réduire le bruit dans la cabine. Un modèle analytique a été créé et validé à l'aide de Matlab pour calculer la Densité Spectrale de Puissance (DSP) de l'accélération, qui est proportionnelle à la Puissance Acoustique Rayonnée (PAR). Une étude de sensibilité paramétrique a été réalisée, afin de déterminer la variation de la DSP de l'accélération, en relation aux sept différents paramètres du panneau : épaisseur du panneau, la densité du matériau, la largeur et la longueur du panneau, le module d'élasticité, le coefficient de Poisson, et le coefficient d'amortissement. Une méthode analytique pour optimiser la performance acoustique d'un panneau d'aéronef est présentée, en changeant les propriétés du panneau, afin de réduire la DSP de l'accélération du panneau provoquée par la CLT. Il est montré que l'épaisseur et la densité du panneau sont les paramètres les plus cohérents et les plus susceptibles de réduire la DSP de l'accélération, dans différentes bandes d'octave dans la gamme des fréquences audibles.

Mots-clefs : Optimisation, Réduction du bruit, Puissance Acoustique Rayonnée, Couche Limite Turbulente, Acoustique structurelle

Abstract

The noise and vibration in an aircraft cabin during cruise conditions is mostly caused by external flow excitations from the turbulent boundary layer (TBL). The TBL causes the fuselage panels on the aircraft to vibrate. These vibrations radiate sound energy in the form of noise. Therefore, it is of interest to determine which aircraft panel parameter is most sensitive in decreasing the amount of radiated sound power and how to optimize these parameters to reduce the noise into the aircraft cabin. An analytical model was created and validated using Matlab that calculates the acceleration power spectral density (PSD), which is related to radiated sound power (RSP). A sensitivity study was performed on the panel parameters, to determine the change in acceleration PSD, in relation to change in seven different panel parameters: panel thickness, material density, panel width and length, Elasticity modulus, Poisson's ratio, and damping ratio. An analytical method to optimize an aircraft panel is presented, by changing the panel properties, in order to reduce the acceleration PSD of the panel caused by the TBL. As expected the panel thickness and the panel density are the most consistent, and effective parameters at reducing the acceleration PSD at different octave bands in the human hearing range.

Keywords: Optimization, Noise Reduction, Radiated Sound Power, Turbulent Boundary Layer, Structural Acoustics

---

1 Introduction

The noise and vibration in an aircraft cabin, during cruise conditions, is primarily caused by the external turbulent boundary layer (TBL) [1]. The TBL causes the fuselage panels on the aircraft to vibrate, which radiate sound energy in the form of noise in the cabin. In this context, the objective of the work is to determine which aircraft panel parameter(s) is/are most effective in decreasing the panel's radiated sound power, and how to optimize these parameters to reduce the noise in the aircraft cabin.

Many researchers have studied the prediction of the response of a simple panel due to the TBL. Strawderman and Brand have some of the earliest simulated results for a turbulent flow excited panel vibration [2]. Others have modelled the response of the plate using wavenumber-frequency formulations, or have used finite element and boundary element methods, where the plate is excited by a number of distributed forces having proper spatial and temporal correlations [3, 4, 5, 6].

One approach to calculate the radiated sound power (RSP) of vibrating structures is to use a modal analysis, as done by Roy and Lapi [7]. This approach is necessary when analyzing obscure shapes, but requires great computational power and time, making it difficult to iterate the calculations for optimization routines. Therefore, when looking at simple shapes, like that of a flat panel, analytical computational methods become a better choice. The analytical expressions for RSP can be derived for a given aircraft panel, in terms of the displacement power spectral density (PSD) [1, 8, 9]. The

† Steven.Sonnenberg@carleton.ca
‡ Joana.Rocha@carleton.ca

acceleration PSD is calculated from the displacement PSD, which is proportional to the RSP [9]. The analytical models developed were modified to account for other panel and enclosure combinations [10, 11]. Berry also showed that the same type of analytical analysis was possible for panels with arbitrary boundary conditions [12].

In the present work, an analytical model which calculates the acceleration PSD was developed in Matlab, based on previously developed models by the author [1, 8, 9, 10, 11]. The current study adds a step forward on previous analyzes by the author, by focusing on the use of these models to determine the effects of modifying aircraft panels' properties on the panel acceleration. In addition, an analytical optimization has been applied in order to determine the panel properties to which will result in higher panel acceleration PSD reduction caused by the TBL.

Optimization can be defined as a means to find the best solution among many feasible solutions that are available. Feasible solutions are those that satisfy all the constraints in the optimization problem [13]. An optimization problem can be defined mathematically as [13, 14]:

Minimize:

$$f(x) \tag{1}$$

Subject to:

$$g_i(x) \le 0 \quad i = 1,2,\dots,m < n \tag{2}$$

$$h_j(x) = 0 \quad j = 1,2,\dots,r < n \tag{3}$$

$$x_l \le x \le x_u \tag{4}$$

Where x is a vector of n design variables given by:

$$x = \begin{bmatrix} x_1 \\ x_2 \\ \vdots \\ x_n \end{bmatrix} \tag{5}$$

The function f, g_i and h_j are all differentiable. In the context of this study, $f(x)$ is the equation for acceleration PSD at a single point on the panel for a given frequency. The design variables (the seven panel parameters being investigated) are bounded by the lower and upper limits, x_l and x_u. The constraints in g_i are inequality constraints compared to the equality constraints in h_j. The constraints are functions of the design variables, and there must be less constraints than the number of design variables. For this initial study there are no constraints being used in order to determine general trends when optimizing the seven parameters. However, in future studies these will be the physical constraints of actual materials available for the construction of the panels. These constraints could be considered in future work, for a second phase of the research, since the panel elastic properties are intrinsic to existing materials, and a material with optimum properties obtained independently (i.e. density, elasticity modulus, Poisson's ratio, or damping coefficient) would not result in a realistic solution. If the design variables, between their bounds, can be proven to satisfy all of the constraints, then a feasible region exists. This feasible region is then solved to determine the optimal design variables, which minimize the objective function.

After the optimization problem can be defined, there are many options when it comes to solving the problem. Optimization algorithms are iterative. They begin with an initial guess and then continue to make improved estimates until the program terminates, hopefully when it has converged on a minimum. The process by which the algorithm selects the next estimate is the defining feature of the algorithm. Good algorithms should be robust, efficient and accurate [15] .

There are many free software codes available that can be used for optimization. The optimizing code used throughout this study is an add-on to Matlab. It uses an interior point algorithm for a nonlinear equation. The equations being analyzed are not linear functions, therefore no linear optimization equation could be used. An interior point algorithm is an approach to constrained minimization by solving a sequence of approximate minimization problems [16]. The name interior point methods means the iterations lie in the interior of the feasible region. This is different from the simplex method, which moves its iterations along the boundary of the feasible region from one extreme point to another [17]. Over the past 30 years interior point methods have been advanced, following the work by Karmarkar [18]. Many books have been written explaining the basics of the method, and the applications it has for both linear and nonlinear functions [19, 17, 20]. This type of algorithm has been used to solve for: optimal electrical power systems, shakedown analysis of pavements and power flow unsolvability [21, 22, 23]. The algorithm can be used in many types of applications and therefore it was selected as a way to obtain initial optimized design variables. In this work, this algorithm has been used to find the minimum acceleration PSD given seven panel parameters.

2 Methodology

The panel is assumed to be flat and simply supported on all four sides. A panel, in the context of an aircraft, might not be defined as the boundary of a sheet of material, but instead as the enclosed area on that sheet, between the stringers and the formers. The connections of the material to the stringers and formers cause that section of material to act as a single, simply supported panel. The vibration of a single panel can be defined as [1]:

$$w(x,y,t) = \sum_{m_x=1}^{Mx} \sum_{m_y=1}^{My} \alpha_{m_x}(x)\beta_{m_y}(y)\, q_{m_x m_y}(t) \tag{6}$$

α_{m_x} and $\beta_{m_y}(y)$ are spatial functions that define the variation in vibration and can be defined as follows, for a simply supported plate [1]:

$$\alpha_{m_x}(x) = \sqrt{\frac{2}{a}}\sin\left(\frac{m_x \pi x}{a}\right) \tag{7}$$

$$\beta_{m_y}(y) = \sqrt{\frac{2}{b}}\sin\left(\frac{m_y \pi y}{b}\right) \tag{8}$$

Where:

a = Panel Length [m]
b = Panel Width [m]
(m_x, m_y) = Plate Mode
$M = Mx * My$ = Total Number of Plate Modes Considered

The first step to calculating the acceleration PSD is to determine the panel modes and the natural frequency that corresponds with each mode, as follows [10]:

$$\omega^P_{m_x m_y} = \sqrt{\frac{1}{\rho_p h_p}\{D_p\left[\left(\frac{m_x\pi}{a}\right)^2 + \left(\frac{m_y\pi}{b}\right)^2\right]^2 + N_x\left(\frac{m_x\pi}{a}\right)^2 + N_y\left(\frac{m_y\pi}{b}\right)^2\}} \tag{9}$$

Where:

$$D_p = \frac{E_p h_p^3}{12(1-\nu_p^2)} \tag{10}$$

ρ_p = Panel Density [kg/m^3]
h_p = Panel Thickness [m]
ν_p = Poisson Ratio
N_x = Panel Longitudinal Tension [N/m]
N_y = Panel Lateral Tension [N/m]
E_p = Panel Elasticity Modulus [Pa]
D_p = Panel Bending Stiffness [Nm]

The dispersion equation (9) applies to a pressurized fuselage which will be analyzed in the future however, this equation can be simplified to assume that the panel is not under tension in either direction, which is the same assumption used for the validation case, in this study. This simplified equation can be seen below [10]:

$$\omega^P_{m_x m_y} = \sqrt{\frac{D_p}{\rho_p h_p}}\left[\left(\frac{m_x\pi}{a}\right)^2 + \left(\frac{m_y\pi}{b}\right)^2\right] \tag{11}$$

In order to determine how many modes are needed at a specific frequency, a convergence test must be completed. Convergence is reached when the distance between two nodes of the structural mode shape is less than, or equal to, half-wavelength, $\lambda/2$, of the bending wave on the plate at the analysis frequency [10]. These values must be rounded to the next highest whole number, to coincide with a plate modal number [10]:

$$N_{Max} = 2a/\lambda \tag{12}$$

$$M_{Max} = 2b/\lambda \tag{13}$$

$$\lambda = 2\pi\omega^{-0.5}\left(\frac{D_p h_p}{\rho_p}\right) \tag{14}$$

The convergence test determines the point at which additional panel modes does not change the overall shape of the final plot, but instead, appears to make the plot slightly noisier. By running a convergence test at every target frequency, it allows the program to limit the number of panel modes used for lower target frequencies, speeding up the computational time to run the program.

Rocha's Research is able to reduce a "coupled system governing equations into the following matrix form" [1]:

$$\begin{bmatrix} M_{pp} & 0 \\ M_{cp} & M_{cc} \end{bmatrix}\begin{Bmatrix} \ddot{q}(t) \\ \ddot{r}(t) \end{Bmatrix} + \begin{bmatrix} D_{pp} & 0 \\ 0 & D_{cc} \end{bmatrix}\begin{Bmatrix} \dot{q}(t) \\ \dot{r}(t) \end{Bmatrix} + \begin{bmatrix} K_{pp} & K_{pc} \\ 0 & K_{cc} \end{bmatrix}\begin{Bmatrix} q(t) \\ r(t) \end{Bmatrix} = \begin{Bmatrix} P_{tbl}(\omega) \\ 0 \end{Bmatrix} \tag{15}$$

This equation can be written as follows [1]:

$$Y(\omega) = H(\omega)X(\omega) \tag{16}$$

$$Y(\omega) = \begin{Bmatrix} W(\omega) \\ P(\omega) \end{Bmatrix} \tag{17}$$

$$X(\omega) = \begin{Bmatrix} P_{tbl}(\omega) \\ 0 \end{Bmatrix} \tag{18}$$

$$H(\omega) = \begin{bmatrix} -\omega^2 M_{pp} + i\omega D_{pp} + K_{pp} & K_{pc} \\ -\omega^2 M_{cp} & -\omega^2 M_{cc} + i\omega D_{cc} + K_{cc} \end{bmatrix}^{-1} \tag{19}$$

This matrix form assumes that the panel is simply supported, and encloses a cavity (like the panels surrounding the enclosed cabin of the aircraft). In this study, the approach taken to analyze the panel does not include the attached chamber since the objective is to compare panel parameters and not cavity parameters. Since the equation must be derived for only the panel, the equation can be reduced to:

$$H_w(\omega) = H(\omega) = \left[-\omega^2 M_{pp} + i\omega D_{pp} + K_{pp}\right]^{-1} \tag{20}$$

Where [1]:

$$M_{pp} = diag[\rho_p h_p] \quad = \text{Mass Matrix} \tag{21}$$

$$D_{pp} = diag[2\rho_p h_p \omega_m \zeta_p] \quad = \text{Damping Matrix} \tag{22}$$

$$K_{pp} = diag[\rho_p h_p \omega_m^2] \quad = \text{Stiffness Matrix} \tag{23}$$

Each of these matrices are of the size MxM. With this information, $S_{ww}(\omega)$ Matrix can be defined as follows [1]:

$$S_{ww}(\omega) = H_w^*(\omega)S_{tbl}(\omega)H_w^T(\omega) \tag{24}$$

In this equation, $S_{tbl}(\omega)$ is a generalized PSD Matrix of the TBL excitation, which has been derived into an analytical equation in Rocha's research, to allow for quick evaluation [1]. With this Displacement PSD Matrix, the Displacement PSD at a single point (taken to be the centre of the panel in all calculations for this study) can be calculated for a given frequency as follows [1]:

$$S_{WW}(x_1, y_1, x_2, y_2, \omega) = \sum_{m_{x_1}, m_{x_2}=1}^{M_x^2} \sum_{m_{y_1}, m_{y_2}=1}^{M_y^2} \alpha_{m_{x_1}}(x_1) * \alpha_{m_{x_2}}(x_2) * \beta_{m_{y_1}}(y_1) * \beta_{m_{y_2}}(y_2) * S_{ww}(\omega)_{m_1, m_2} \tag{25}$$

The equations required to calculate the Velocity (S_{VV}) and the Acceleration PSD (S_{AA}), at a single point on the panel are as follows [9]:

$$S_{VV} = \omega^2 * S_{WW} \tag{26}$$
$$S_{AA} = \omega^4 * S_{WW} \tag{27}$$

To show that calculating either S_{WW}, S_{VV}, or S_{AA} will give direct correlations to how it effects the RSP of a panel, the basic equations required to calculate RSP have been provided [8, 24]:

$$RSP(x_1, y_1, x_2, y_2, \omega) = \sum_{m_{x_1}, m_{x_2}=1}^{M_x^2} \sum_{m_{y_1}, m_{y_2}=1}^{M_y^2} \psi_{m_{x_1}}(x_1) * \psi_{m_{x_2}}(x_2) \; \phi_{m_{y_1}}(y_1) * \phi_{m_{y_2}}(y_2) * \prod(\omega)_{m_1, m_2} \tag{28}$$

$$\prod(\omega) = S_{VV} * M(\omega) \tag{29}$$

$$M(\omega) = 8\frac{\rho_0}{c_0}\left(\frac{\omega ab}{\pi^3 m_x m_y}\right)^2 \int_0^{\pi/2}\int_0^{\pi/2} \left\{\frac{\frac{cos}{sin}\left(\frac{\alpha}{2}\right)\frac{cos}{sin}\left(\frac{\beta}{2}\right)}{\left[\left(\frac{\alpha}{m_x\pi}\right)^2 - 1\right]\left[\left(\frac{\beta}{m_y\pi}\right)^2 - 1\right]}\right\}^2 \sin\theta \, d\theta d\emptyset \tag{30}$$

These equations show that the RSP is related to S_{VV}, so that any conclusions made from the sensitivity study on S_{AA}, will be related to the RSP. This allows for meaningful conclusions to be made about RSP without having to run a more time intensive program.

3 Results

A sensitivity study was performed on seven panel parameters, to determine which parameter is most effective at reducing the acceleration PSD in select octave bands. The parameters were varied individually while maintaining the other variables at their initial values, and the changes in the acceleration PSD in each of the octave bands were analyzed. In the present study, no constraints have been considered (one parameter relative to another), in order to determine the general trends when optimizing each of the seven individual parameters. Future work could consider these constraints. The following octave bands (in the human hearing range) have been analyzed: 89.1-178 Hz, 178-355 Hz, 355-708 Hz and 708-1410 Hz. The sensitivity study was run for seven parameters: thickness, material density, panel width and length, elastic modulus, Poisson's ratio and damping ratio.

Table 1 contains the initial panel parameters used in the sensitivity study and Figure 1 to Figure 4 contain the sensitivity studies, for each of the octave bands.

Table 1: Initial panel parameters for optimization.

Variable	Value
Length	0.46 m
Width	0.33 m
Thickness	0.0048 m
Elasticity Modulus	$6.5 * 10^{10}$ Pa
Density	1.225 kg/m^3
Poisson's Ratio	0.3
Damping Ratio	0.01

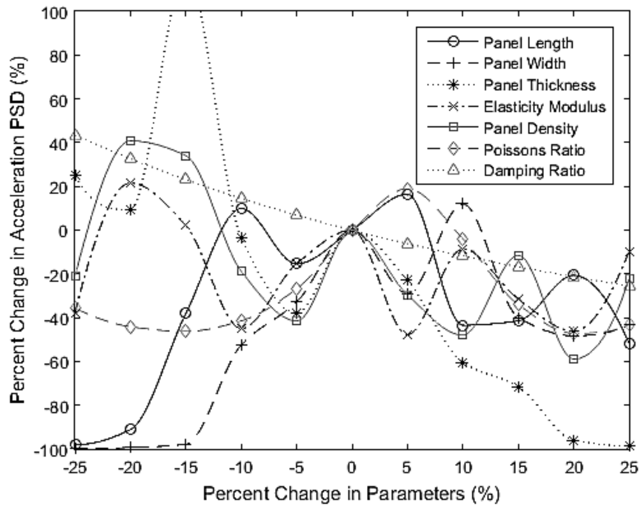

Figure 1: Percent change in acceleration PSD versus percent change in panel parameter for octave 89.1-178 Hz with limited Y-axis extents.

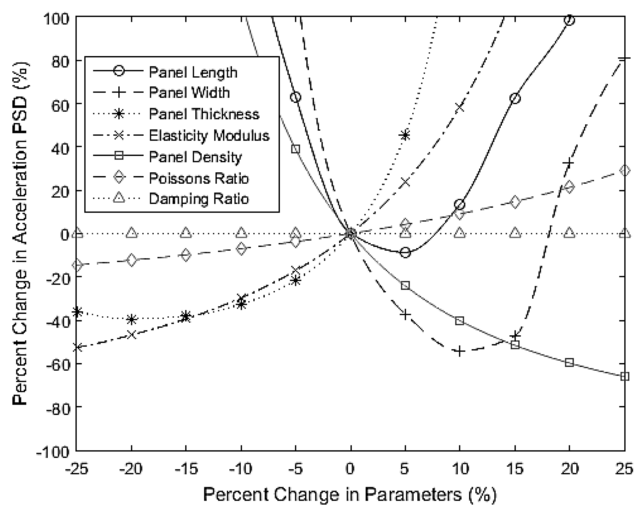

Figure 2: Percent change in acceleration PSD versus percent change in panel parameter for octave 178-355 Hz with limited Y-axis extents.

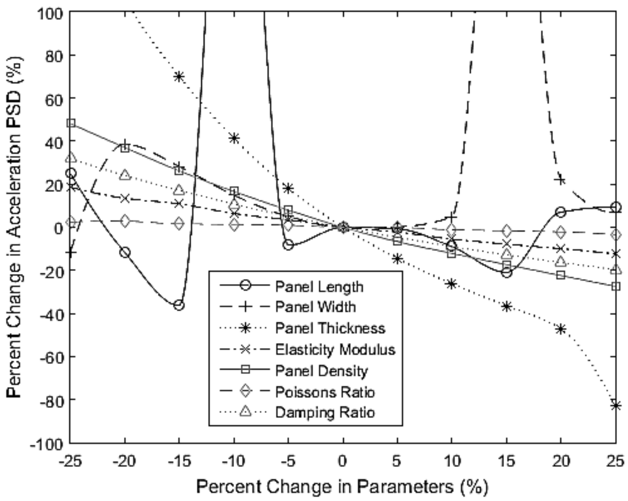

Figure 3: Percent change in acceleration PSD versus percent change in panel parameter for octave 355-708 Hz with limited Y-axis extents.

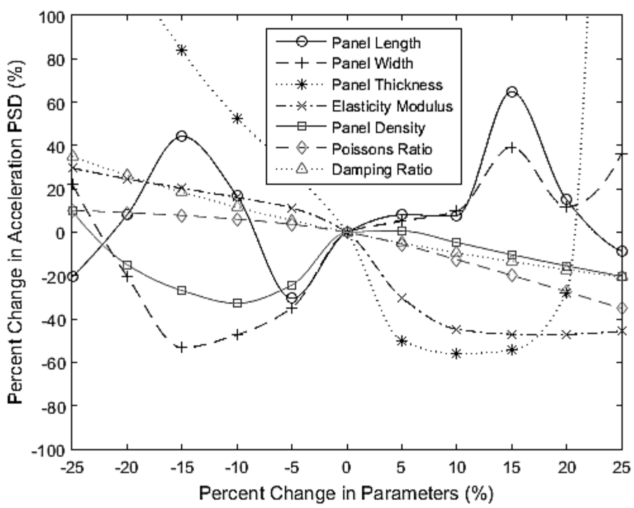

Figure 4: Percent change in acceleration PSD versus percent change in panel parameter for octave 708-1410 Hz with limited Y-axis extents.

It can be seen from Figure 1 that there is a very low correlation between change in panel parameters and change in acceleration PSD at frequencies, between 89.1-178 Hz. This could be due to the low number of panel modes existent at low frequencies. This can be seen as well from the convergence criteria [10], when one observes that decreasing the frequency, less panel modes are required to achieve convergence. When the parameters are modified at these lower frequencies, it allows for the convergence test to result in values less than one. Therefore, the octave band 89.1-178 Hz will be ignored when determining which panel parameter is most sensitive to changing the acceleration PSD.

As shown in Figure 2 to Figure 4, both the panel width and length have fluctuating values. These fluctuations are believed to occur because the panel width and length are main components of calculating $S_{tbl}(\omega)$. The variables are located within sinusoidal functions, with the change in these parameters being non-linear. For this reason, these parameters cannot be defined by a simple trend, and therefore, are not the most sensitive at reducing the overall acceleration PSD.

It was found that the two parameters that are the most effective for reducing the average acceleration PSD, within the different octave bands, are panel thickness and panel density, as these two parameters have the steepest slopes. As the thickness is increased, the higher frequency noise is reduced, as expected. However it has less effect on the lower frequency (longer wavelength) signals. Even though the panel density has more gradual slopes in comparison to the panel thickness, the trend is more consistent across all of the analyzed octave bands. Hence, it is likely that panel density is the most sensitive at reducing the overall noise across the human hearing range, whereas thickness may be the most sensitive at reducing the noise at certain octave bands.

The analysis was then modified to determine the optimal panel parameters that resulted in the smallest average acceleration PSD over the octave band. The analysis is used to optimize each of the seven parameters individually, and concurrently. Since the general trend of the sensitivity studies predicts that the minimum acceleration PSD is reached when both the thickness and the density are maximized to the upper constraint, optimizing these parameters individually simply results in the upper constraint. Therefore, it is of more interest to determine if there is a correlation between the octave band and the panel length. Figure 5 shows the optimal panel length at the center frequency, of different octave bands, and compares these values to the calculated flexural wavelength, convective wavelength and acoustic wavelength, at the same frequencies.

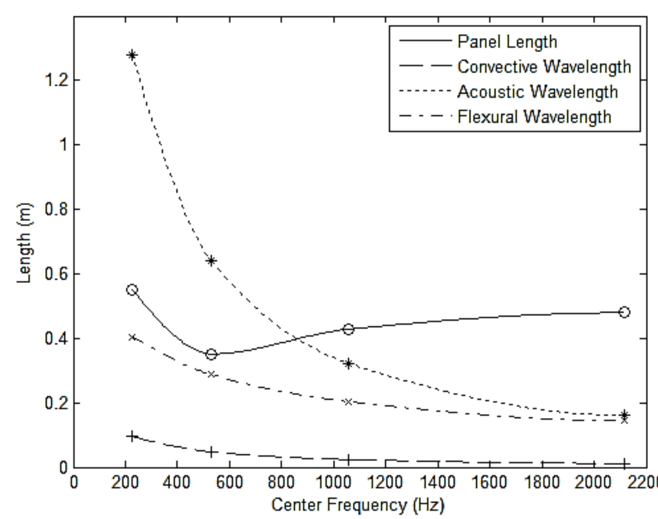

Figure 5: Optimal panel length at the center frequency of different octave bands that result in a local minimum average acceleration PSD compared to the calculated flexural wavelength, convective wavelength and acoustic wavelength.

It was predicted that the optimal panel length would be related the flexural wavelength, convective wavelength and acoustic wavelength; however, Figure 5 does not support this hypothesis. The optimization routine currently finds local minimums in the constrained space, rather than the global minimum. It also shows that by averaging over an entire octave band it becomes difficult to see the exact correlation between the panel length and the frequency.

Two modifications to this approach were then taken to get a better understanding of the relationship between frequency and optimal panel length. The first change was to modify the optimizing routine, to ensure that the overall global minimum was being determined, and to ensure the resulting length was not just the location of a local minimum occurring at some multiple of the wavelength. The second modification was to calculate the optimal panel length, for a single frequency, instead of over an entire octave band. This allows for a more detailed curve to be plotted for length versus frequency. Figure 6 shows the result of this new optimization study, over the first two octave bands previously investigated.

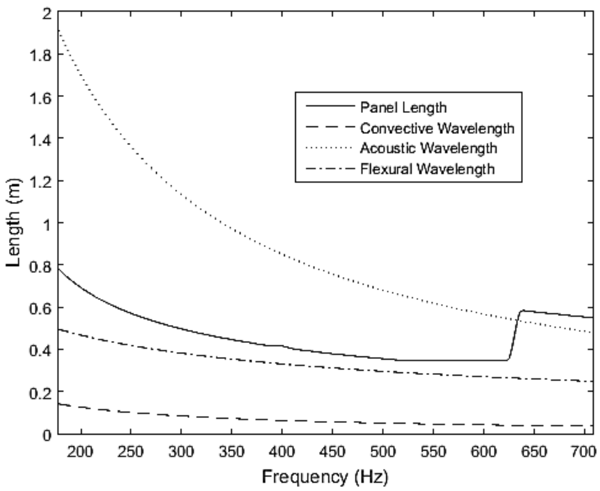

Figure 6: Optimal panel length at individual frequencies that result in a global minimum average acceleration PSD compared to the calculated flexural wavelength, convective wavelength and acoustic wavelength for two octave bands.

Figure 6 shows that there are additional panel lengths that result in local minimum acceleration PSDs and that the optimal panel length that results in the true global minimum, follows the same exponential decay as the flexural wavelength, convective wavelength and acoustic wavelength. From 178 Hz to 500 Hz the global minimum acceleration PSD is found at panel lengths that follow the expected exponential decay. From 500 Hz to 625 Hz the optimization routine levels off at the lower bound of the design space for the optimization routine. The lower bound was decreased as low as it could while running this routine. The lower bound cannot be decreased any farther because of the convergence test. If the panel length is set too small, the convergence test results in a very small number. This means only a few panel modes are used to calculate the acceleration PSD. This causes inaccurate values to be predicted for the acceleration PSD and skews the optimization data. From 625 Hz to 708 Hz there is a shift in the plot. Since the true global minimum would be found below the lower bound of the integration, the optimizing routine finds a local minimum which is now smaller than the acceleration PSD at the lower bound. The local minimum found is approximately equal to two times the expected global minimum. Therefore, there are local minimums at multiples of the optimal panel length.

Figure 7 shows the result of the optimization study, over the four octave bands.

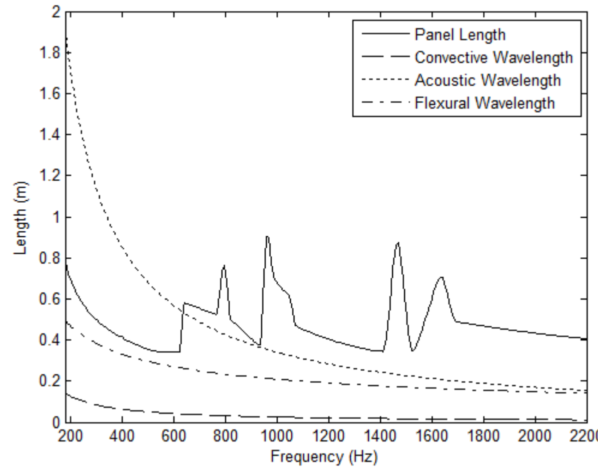

Figure 7: Optimal panel length at individual frequencies that result in a global minimum average acceleration PSD compared to the calculated flexural wavelength, convective wavelength and acoustic wavelength for four octave bands.

From Figure 7 it can be seen that, at certain frequencies, the optimizing model does not find global minimums at lengths which correlate with the convective, acoustic or flexural wavelengths. These regions also coincide with the peaks in the acceleration PSD for the lengths in this study (these same peaks are observed in Rocha's earlier work, associated to the "Validation Case 2" in Figure 5 [1]). At these regions, the peaks shift as the panel length changes making it difficult to determine an optimal panel length. It is found that the length at which the peak shifts farthest away, and not converging to the length that has minimized the amplitude of the peak. However, by moving away from these regions, the lengths still follow the same exponential decay as the convective, acoustic and flexural wavelengths at multiples of the expected optimal panel lengths.

4 Conclusion

An optimization study is presented, with the objective to reduce the acceleration PSD of a panel excited by a TBL by optimizing the panel's length. It has been shown that the optimal panel length that results in the true global minimum, follows the same exponential decay as the flexural wavelength, convective wavelength and acoustic wavelength. It has also been shown that at multiples of the optimal panel length local minimum acceleration PSDs occur. The sensitivity study indicates that panel thickness and panel density are the most consistent, and effective parameters at reducing the acceleration PSD at different octave bands in the human hearing range.

The next step of this research would be to see if the optimal panel width is also a function of the flexural wavelength, convective wavelength and acoustic wavelength. It would also be of interest to continue the sensitivity study into the higher octave bands to determine if panel thickness and density are still the most consistent, and effective parameters at reducing the acceleration PSD.

The optimization model described in the current paper will be useful in the earlier stages of aircraft design, by helping the designer to select panel configurations that reduce the amount of noise due to the TBL inside the cabin of the aircraft.

References

[1] J. Rocha, A. Suleman and F. Lau, "An accurate Coupled Structural- Acoustic Analytical Framework for the Prediction of Random and Flow-Induced Noise in Transport Vehicles: Its Validation," *Canadian Acoustics,* vol. 37, no. 3, 2009.

[2] W. A. Strawderman and R. S. Brand, "Turbulent-flow-excited vibration of a simply supported, rectangular flate plate," *The Journal of the Acoustical Society of America,* vol. 45, no. 1, pp. 177-192, 1969.

[3] C. Maury, P. Gardonio and S. J. Elliot, "A number approach to modelling the response of a randomly excited panel, part i: General theory," *Journal of Sound and Vibration,* vol. 252, no. 1, pp. 83-113, 2002.

[4] C. Maury, P. Gardonio and S. J. Elliott, "A wavenumber approach to modelling the response of a randomly excited panel, part ii: Application to aircraft panels excited by a turbulent boundary layer," *Journal of Sound and Vibration,* vol. 252, no. 1, pp. 115-139, 2002.

[5] N. H. Schiller, "Decentralized control of sound radiation from periodically stiffened panels," Virginia Polytechnic Institute and State University, Blacksburg, Virginia, 2007.

[6] J. M. Montgomery, "Modelling of aircraft structural-acoustic response to complex sources using coupled fem-bem analyses," *Collection of Technical Papers - 10th AIAA/CEAS Aeroacoustics Conference,* vol. 1, pp. 266-274, 2004.

[7] N. Roy and M. Lapi, "Efficient Computation of the Radiated Sound Power of Vibrating Structures using a Modal Approach," in *Acoustics*, Paris, 2008.

[8] J. Rocha and D. Palumbo, "On the Sensitivity of Sound Power Radiated by Aircraft Panels to Turbulent Boundary Layer Parameters," *Journal of Sound and Vibrations,* vol. 331, pp. 4785-4806, 2012.

[9] J. Rocha, "Sound Radiation and Vibration of Composite Panels Excited by Turbulent Flow: Analytical Prediction and Analysis," *Shock and Vibration,* vol. 2014, no. 316481, pp. 1-18, 2014.

[10] J. Rocha, A. Suleman and F. Lau, "Turbulent Boundary Layer Induced Noise and Vibration of a Multi-Panel Walled Acoustic Enclosure," *Canadian Acoustics,* vol. 38, no. 4, pp. 9-22, 2010.

[11] J. Rocha, A. Suleman and F. Lau, "Prediction of Turbulent Boundary Layer Induced Noise in the Cabin of a BWB Aircraft," *Shock and Vibration,* vol. 19, pp. 693-705, 2012.

[12] A. Berry, J.-L. Guyader and J. Nicolas, "A general formulation for the sound radiation from rectangular, baffled plates with arbitrary boundary conditions," *Journal of the Acoustical Society of America,* vol. 88, no. 6, pp. 2792-2802, 1990.

[13] R. K. Arora, Optimization: algorithms and applications, Chapman and Hall, 2015.

[14] U. Diwekar, Introduction to Applied Optimization, New York: Springer, 2008.

[15] J. Nocedal and S. J. Wright, Numerical Optimization, New York: Springer, 2006.

[16] MathWorks, "Contrained Nonlinear Optimization Algorithms," MathWorks, [Online]. Available: http://www.mathworks.com/help/optim/ug/constrained-nonlinear-optimization-algorithms.html#brnox0o. [Accessed 18 May 2016].

[17] L. Yong, "Interior Point Algorithms and Applications," *Future Intelligent Information Systems,* no. 86, pp. 165-172, 2011.

[18] N. Karmarkar, "A new polynomial-time algorithm for linear programming," *Combinatorica,* vol. 4, no. 4, pp. 373-395, 1984.

[19] C. Roos, T. Terlaky and J.-P. Vial, Interior Point Methods for Linear Optimization, New York: Springer, 2005.

[20] L. Luksan, C. Matonoha and J. Vlcek, "Interior point methods for large-scale nonlinear programming," *Optimization Methods and Software,* vol. 20, no. 5, pp. 569-582, 2005.

[21] M. E. El-Hawary and I. A. Farhat, "Interior point methods application in optimum operational scheduling of electric power systems," *IET Generation, Transmission and Distribution,* vol. 3, no. 11, pp. 1020-1029, 2009.

[22] A. D. Nguyen, A. Hachemi and D. Weichert, "Applications of the interior-point method to shakedown analysis of pavements," *International Journal for Numerical Methods in Engineering,* no. 75, pp. 414-439, 2008.

[23] S. Granville, J. C. Mello and A. C. Melo, "Application of interior point methods to power flow unsolvability," *IEEE Transactions on Power Systems,* vol. 11, no. 2, pp. 1096-1103, 1996.

[24] C. Wallace, "Radiation resistance of a rectangular panel," *The Journal of the Acoustical Society of America,* vol. 51, no. 3, pp. 946-952, 1972.

[25] C. S. Beightler and D. J. Wilde, Foundations of Optimization, Englewood Cliffs, N.J.: Prentice-Hall, 1967.